Pramana – J. Phys. (2018) 90:61
https://doi.org/10.1007/s12043-018-1552-y

Optimum parameters controlling distortion and noise of semiconductor laser under analog multichannel modulation

ALAA MAHMOUD[1,*], MOUSTAFA AHMED[2] and SAFWAT W Z MAHMOUD[2]

[1]Laser Institute for Research and Applications (LIRA), Beni-Suef University, 62511 Beni-Suef, Egypt
[2]Department of Physics, Faculty of Science, Minia University, 61519 Minia, Egypt
*Corresponding author. E-mail: alaa.abutaleb@lira.bsu.edu.eg

MS received 25 September 2017; revised 20 November 2017; accepted 22 November 2017; published online 3 April 2018

Abstract. This paper presents a comprehensive modelling and simulation study on the optimum parameters that control the distortion and noise of semiconductor lasers (SLs) subject to multichannel modulation for use in analog cable television (CATV) fibre links. The study is based on numerical integration of the rate equation model of the semiconductor laser. The parameters comprise the modulation index per channel (m/ch), number of loaded channels (N) and fibre length (L_F). The signal distortions include the composite second-order (CSO) and composite triple beat (CTB) distortions. The noise is assessed in terms of the relative intensity noise (RIN) and carrier-to-noise ratio (CNR). In order to achieve acceptable CNR values for SL, m/ch should be less than 7.5 and 2% when loading 12 and 80 channels, respectively. For the CATV fibre link with $L_F = 10$ km, the increase in the number of channels from 12 to 80 corresponds to lowering the optimum value of m/ch from 7 to 1%. The increase of L_F to 50 km limits the optimum value of m/ch between 1.4 and 1%, which corresponds to loading between 12 and 17 channels only.

Keywords. CATV fibre link; distortion; noise; semiconductor laser; multichannel modulation.

PACS Nos **42.55.Px; 42.81.Cn; 42.30.Lr; 42.60.Mi**

1. Introduction

The demand for analog transmission of TV channels through optical fibre links has grown dramatically due to their lower cost and compatibility with current TV sets, compared to the digital transmission [1]. A CATV fibre link typically consists of a laser diode transmitter, an optical fibre and a photodetector receiver. The channels, in the electrical analog signals form, are transferred into the optical domain using semiconductor laser (SL) and are then coupled to the optical fibre. After some length of the fibre, the signals are transferred back into the electrical domain by means of a photodiode [2]. SLs are characterised by interesting features, such as low power requirements, high efficiency, compact size emitting very narrow beam of light and facility of direct modulation [3]. The use of directly modulated SLs gives many necessary characteristics such as simplicity and cost-effective solutions compared with external modulation techniques. However, directly modulated SLs may present nonlinear distortions and high-intensity noise due to their nonlinear characteristics [4,5]. These drawbacks limit the transmission performance of both the laser and CATV fibre link. In addition, the fibre link performance restrictions can come from photodetector characteristics.

Nonlinear distortions in the modulated laser signal originate from the intrinsic nonlinear fluctuations of the electron and photon densities in the active region of the laser [4]. In multichannel systems, such as CATV systems, when the TV channels are combined and applied as input signals, a lot of nonlinear distortions in the laser output are created, resulting in very high levels of interference at certain channel frequencies. These products form the so-called 'composite second-order (CSO)' distortions and 'composite triple beat (CTB)' distortions [6,7]. CSO is the sum of the second-order non-linear distortions on a given channel [2,8], whereas a lot of third-order intermodulation products generate composite distortions, measured by CTB [9]. Degradation of CSO below –55 dBc and CTB below –65 dBc cause the TV picture to have undesired tilted lines or swimming strips, respectively [6–8,10,11].

On the other hand, SLs are intrinsically noisy [12]; their output exhibits fluctuations in both phase and intensity. The main source of this noise is the spontaneous

emission process [12]. Photodetector noise sources are also important factors in the evaluation of the noise performance of the CATV fibre link; namely, shot and thermal noises. The total noise performance of the CATV fibre link is assessed in terms of CNR. The CNR is the ratio of the fundamental TV channel's power to the noise floor in specified bandwidth centred within the channel frequency under test [1,2]. In order to avoid interference of the noise floor with the TV signal, or the so-called 'snow' that can overwhelm the picture resolution and contrast [7,13], CNR should exceed 50 dBc [1,6,10].

It is practically important to determine the optimum modulation conditions and design parameters of the CATV fibre link that are required to yield simultaneously accepted values of CSO, CTB and CNR that result in high-quality pictures and high channel capacity [5]. However, computationally, the optimisation of the link parameters is not an easy task [10]. The modulation conditions and design parameters of the link include the modulation index per channel m/ch, number of loaded channels N and fibre length L_F. The modulation index should be fundamentally limited to avoid the laser nonlinear distortions [5,10,11,14]. However, this index is desired to be as large as possible to decrease the negative impact of the laser noise [2,6,10,15]. The number of loaded channels and fibre length also play important roles in the assessment of both distortion and noise effects in multichannel systems [13,16,17].

In this paper, we present comprehensive modelling and simulation on the distortion and noise of SLs and CATV fibre links subject to multichannel modulation. The aim of this study is to optimise the modulation conditions and structure parameters of the link. The channel frequencies are distributed according to the analog downstream band of the national television standards committee (NTSC) [2]. The study is based on the rate equation model of SLs in [18]. We determine the optimum ranges of m/ch for different numbers N of loaded channels that correspond to accepted values of CSO, CTB and CNR using different fibre lengths. We also investigate the individual contributions of the noise sources in terms of CNR as a function of the modulation parameters. The results showed that the optimum values of m/ch vs. the number N of loaded channels are controlled by CNR. On the other hand, the optimum values for the CATV fibre link are determined by both the CSO and CTB distortions. When $L_F = 10$ km, the increase in the number of channels from 12 to 80 corresponds to lowering the optimum value of m/ch from 7 to 1. The increase of L_F to 50 km limits the optimum value of m/ch between 1.4 and 1%, which corresponds to loading between 12 and 17 channels only.

2. Theoretical and calculation model

The dynamics and modulation characteristics of SLs are simulated by numerical integration of the following rate equations of the injected carrier density $N(t)$ and photon density $S(t)$ using modulation current $I(t)$ [18]:

$$\frac{\mathrm{d}N(t)}{\mathrm{d}t} = \frac{I(t)}{eV} - \frac{N(t)}{\tau_c} - \frac{g_0(N(t)-N_0)}{1+\varepsilon S(t)}S(t) + F_N(t), \tag{1}$$

$$\frac{\mathrm{d}S(t)}{\mathrm{d}t} = \frac{\Gamma g_0(N(t)-N_0)}{1+\varepsilon S(t)}S(t) - \frac{S(t)}{\tau_p} + \frac{\Gamma\beta N(t)}{\tau_c} + F_S(t), \tag{2}$$

where e is the electron charge, V is the volume of the active region, τ_c is the electron lifetime, τ_p is the photon lifetime, and β is the fraction of spontaneous emission noise coupled into the lasing mode. The third term in eq. (1) and first term in eq. (2) describe the optical gain, which influences the modulation response of the laser [19,20]. g_0 is the differential gain coefficient, N_0 is the carrier density at transparency, Γ is the confinement factor and ε is the gain suppression factor. The last terms $F_N(t)$ and $F_S(t)$ are Langevin noise sources with Gaussian probability distributions and are added to the rate equations to account for intrinsic fluctuations of the laser [21]. The power P of light emitted from the laser is calculated from the emitted photon density $S(t)$ using the relationship [18]

$$P(t) = \frac{V\eta h\nu}{2\Gamma\tau_p}S(t), \tag{3}$$

where ν is the optical frequency, h is the Planck's constant, and η is the differential quantum efficiency. The power spectrum $p(f)$ of the modulated laser signal output is calculated using the fast Fourier transformation (FFT) as

$$p(f) = \sqrt{\frac{\Delta t}{T}}\,|\mathrm{FFT}(P(t))|\,, \tag{4}$$

where Δt is the time integration step and T is the time period.

The injection current $I(t)$ in eq. (1) is denoted by [22]

$$I(t) = I_b + I_m \times \psi_{\mathrm{m}}(t), \tag{5}$$

where I_b is the bias current, I_m is the modulation current, and $\psi_{\mathrm{m}}(t)$ indicates the shape of the current signal. For the analysis of analog modulation, it is convenient to consider sinusoidal modulation at TV channel frequency f_m with amplitude A. Hence, the shape of the

current signal for multichannel modulation is given by [22]

$$\psi_m(t) = \sum_{i=1}^{N} A \sin(2\pi f_{mi} t), \tag{6}$$

where N is the number of channels.

The measure of the amount of the modulation signal affecting the light output is evaluated in terms of the so-called 'modulation index (m)', which is defined as [6]

$$m\% = \frac{A \times I_m}{I_b} \times 100. \tag{7}$$

Under multichannel modulation, each channel is modulated by an equal modulation index called 'modulation index per channel (m/ch)', which is determined for each number N of the channels loaded as

$$m/ch = \frac{m}{\sqrt{N/2}}; \quad N \geq 10. \tag{8}$$

It is worth noting that the present amplitude modulation causes changes in both the refractive index and optical phase of the SL, which induce frequency chirping. The associated phase noise and frequency chirp are not of interest in the present case of evaluating the CATV link performance in terms of intensity noise and distortion.

2.1 *Procedures of distortion calculation*

First the SL is modulated under the simple case of two-channel modulation, and the second-order intermodulation distortion (IMD2) and third-order intermodulation distortion (IMD3) generated in the optical signal are determined. For modulation frequencies f_{m1} and f_{m2}, IMD2 and IMD3 are calculated using the power spectrum $p(f)$ of the laser signal as the differences between the TV channel's carrier powers and the second and third higher intermodulation products at ($f_{m1} + f_{m2}$ or $f_{m2} - f_{m1}$) and ($2f_{m1} - f_{m2}$ or $2f_{m2} - f_{m1}$), respectively [23]. Next, under the multichannel modulation, the number of the generated second-order distortion product (N_{COS}) and third-order distortion product (N_{CTB}), are decided. Then, the values of CSO and CTB distortions are calculated, respectively, as [2,6,8,14,24]

$$\mathrm{CSO} = \mathrm{IMD2} + 10\log(N_{\mathrm{CSO}}) \tag{9}$$

$$\mathrm{CTB} = \mathrm{IMD3} + 10\log(N_{\mathrm{CTB}}) + 6. \tag{10}$$

For any system of equally spaced carrier frequencies, such as the NTSC modulation system, N_{COS} and N_{CTB} can be determined empirically as [6,9]

$$N_{\mathrm{CSO}}(\text{below carrier}) = (N-1)\left[1 - \frac{f_m - \Delta f}{f_H - f_L}\right], \tag{11}$$

$$N_{\mathrm{CSO}}(\text{above carrier}) = (N-1)\left[\frac{f_m - 2f_L + \Delta f}{2(f_H - f_L)}\right], \tag{12}$$

$$N_{\mathrm{CTB}} = \frac{(N-1)^2}{4} + \frac{(N-M)(M-1)}{2} - \frac{N}{4}, \tag{13}$$

where f_L and f_H are the frequencies of the lowest and the highest frequency channels, respectively, Δf is the carrier spacing, N is the total number of channels, and M is the number of the channel being measured.

2.2 *Procedures of noise calculation*

The Langevin noise sources in rate equations (1) and (2) that account for the generation of laser fluctuations, as well as both the shot and thermal noise sources of the receiver are taken into account. The laser noise is characterised in terms of the frequency spectrum of RIN and its low-frequency level, LF-RIN. The spectrum of RIN is defined as the Fourier transformation of the autocorrelation function of the power fluctuation $\delta P(t)$:

$$\mathrm{RIN} = \frac{1}{\bar{P}^2} \int_0^\infty \delta P(t) \delta P(t+\tau) \mathrm{e}^{j2\pi f \tau} \mathrm{d}\tau, \tag{14}$$

where f is the Fourier frequency. For integration of the rate equations over a long time period T, RIN is calculated as [25]

$$\mathrm{RIN} = \frac{1}{\bar{P}^2} \left\{ \frac{1}{T} \int_0^T \left[\int_0^\infty \delta P(t) \delta P(t+\tau) \mathrm{e}^{j2\pi f \tau} \mathrm{d}\tau \right] \mathrm{d}t \right\}. \tag{15}$$

RIN is evaluated via eq. (15) by applying FFT to the fluctuations $\delta P(t)$ around $\bar{P}$ as [25]

$$\mathrm{RIN} = \frac{1}{\bar{P}^2} \frac{\Delta t^2}{T} \left| \mathrm{FFT}(\delta P(t)) \right|^2. \tag{16}$$

On the other hand, the mean-squared noise powers due to shot noise (N_{sh}) and thermal noise (N_{th}) of the receiver can be modelled mathematically as stationary random processes with Poisson statistics (approximated often by Gaussian statistics) and expressed by [26]

$$N_{\mathrm{sh}} = \left\langle i^2_{\mathrm{shot}} \right\rangle R_{\mathrm{load}} = 2eR_{\mathrm{load}} B \left(I_{\mathrm{ph}} + I_{\mathrm{d}} \right), \tag{17}$$

$$N_{\mathrm{th}} = \left\langle i^2_{\mathrm{thermal}} \right\rangle R_{\mathrm{load}} = 4kBT_k, \tag{18}$$

where $\left\langle i^2_{\mathrm{shot}} \right\rangle$ and $\left\langle \mathrm{i}^2_{\mathrm{thermal}} \right\rangle$ are the autocorrelation functions of the shot and thermal noise currents, respectively, R_{load} is the load resistance, and B is the noise bandwidth. I_{ph} is the photocurrent, which is calculated from the

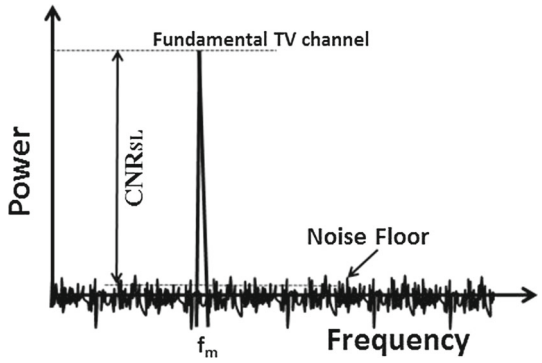

Figure 1. Scheme illustrating calculation of CNR of the laser signal.

receiver responsivity (R) as $I_{\text{ph}}(t) = RP(t)$ [27]. I_d is the dark leakage current, k is the Boltzmann's constant, and T_k is the absolute temperature in Kelvin.

In order to examine the individual contributions of the noise sources in terms of CNR, the values of CNR of both of the laser and photodiode are calculated as the difference between the fundamental TV channel's power and the noise floor in a specified bandwidth (4 MHz [28]) centred within the channel under test [1,2]. Figure 1 illustrates the scheme of calculating the CNR value of the semiconductor laser CNR_{SL}. It is calculated using the relationship

$$\text{CNR}_{\text{SL}} = 10\log_{10}\left(\frac{\text{Fundamental TV channel's power}}{\text{Noise floor}}\right). \tag{19}$$

The total CNR for the CATV fibre link at the optical channel output from the individual CNRs can be expressed by [13,29,30]

$$\text{CNR}_{\text{total}} = 10\log\left(10^{\frac{\text{CNR}_{\text{SL}}}{10}} + 10^{\frac{\text{CNR}_{\text{shot}}}{10}} + 10^{\frac{\text{CNR}_{\text{thermal}}}{10}}\right). \tag{20}$$

The contributions of noise in an optical receiver are $\text{CNR}_{\text{thermal}}$ (due to thermal noise) and CNR_{shot} (due to shot noise).

3. Numerical approach

Rate equations (1) and (2) are numerically integrated by the fourth-order Runge–Kutta method [31] within the frame of simulating SL dynamics using the OptiSystem software. The time integration step is set as short as $\Delta t \sim 5$ ps. An analog downstream band of the NTSC frequency plan in [2] is used with carriers of frequency spans (channel 2: 55.25 ∼ channel 80: 559.25 MHz) at a bandwidth of 6 MHz. The calculations are applied to distributed feedback (DFB) lasers, which are commonly used in the CATV technology [32] along with a single-mode fibre (SMF) [3] and a PIN photodiode [3]. The parameters used in the calculations are listed in table 1.

4. Simulation results and discussion

4.1 *Distortion characteristics*

Figures 2a and 2b plot the CSO and CTB distortions, respectively, vs. the modulation index per channel m/ch for channel 12 (205.25 MHz) under different numbers of channels of $N = 12, 25, 40$, and 80. The figures show that both the CSO and CTB distortions increase with the increase in m/ch and/or N. The dashed lines in the two figures represent the threshold acceptable levels of CSO < -55 dBc and CTB < -65 dBc required to achieve good picture quality as reported in [6–8,10,11].

Influence of the fibre length L_F on the signal distortions is illustrated in figure 3. The figure shows the variation of (a) CSO and (b) CTB distortions with L_F at the accepted value of $m/ch = 2\%$ under the same channel conditions in figures 2a and 2b, respectively. It can be seen that both CSO and CTB distortions increase with the increase in L_F and/or N, the number of channels loaded. For example, in figure 3a the increase in L_F up to 50 km results in the increase of CSO distortion from -71.2 to -50 dBc when $N = 12$, from -66.5 to -45.4 dBc when $N = 40$, and from -59.6 to -38.4 dBc when $N = 80$. On other hand, when L_F increases up to 50 km, the CTB distortion degrades from -85.5 to -64.2 dBc when $N = 12$, from -72.5 to -51.2 dBc when $N = 40$, and from -66.9 to -45.7 dBc when $N = 80$, as shown in figure 3b. The present simulation results for the CSO and CTB distortions agree with the experimental results reported by Lin *et al* [13], and are in good accordance with the experimental findings of CSO by Bergmann *et al* [16].

4.2 *Noise characteristics*

Figure 4 plots the LF-RIN level of the SL as a function of the number of loaded channels N when $m/ch = 7\%$. The three insets (a)–(c) display the frequency spectra of RIN at three distinct channel numbers of $N = 10$ (weak load), 40 (intermediate load), and 80 (strong load), respectively. As shown in the figures, LF-RIN increases with the increase in N. Inset (a) shows that LF-RIN $= -175$ dB/Hz when $N = 10$. The low-frequency noise LF-RIN is calculated by averaging the RIN components in the frequency region of white noise [21]. In

Table 1. Typical values of DFB laser, SMF and PIN photodiode parameters used in the calculations [3,32].

Symbol	Definitions of parameters	Value	Unit
DFB Laser			
λ	Wavelength	1550	nm
V	Active layer volume	1.5×10^{-10}	cm^3
η	Quantum efficiency	0.4	
g_0	Differential gain coefficient	2.5×10^{-16}	cm^2
N_0	Carrier density at transparency	1×10^{18}	cm^{-3}
Γ	Mode confinement factor	0.4	
τ_c	Carrier lifetime	1×10^{-9}	s
τ_p	Photon lifetime	3×10^{-12}	s
β	Spontaneous emission factor	3×10^{-5}	
ε	Gain compression coefficient	1×10^{-17}	cm^3
I_{th}	Threshold current	33.45	mA
I_b	Bias current	60	mA
Optical SMF			
α	Attenuation coefficient	0.2	dB/km
D	Dispersion	16.75	ps/nm/km
L_F	Length	(0–50)	km
PIN photodiode			
R	Responstivity	1	A/W m^{-3}
I_d	Dark current	0	A
N_{th}	Thermal noise	1×10^{-21}	W/Hz
R_{load}	Load resistance	50	Ω

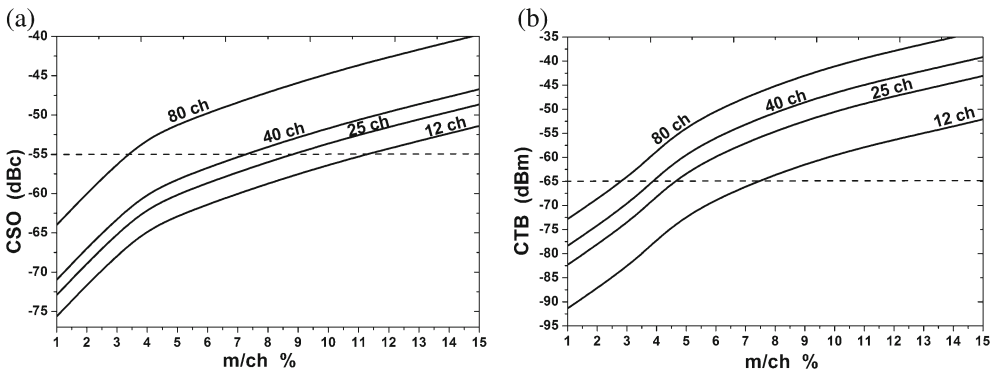

Figure 2. Variation of (**a**) CSO and (**b**) CTB distortions with modulation index per channel m/ch under 12, 25, 40, and 80 channels at ch. 12. The dashed lines represent the threshold acceptable levels.

the present case, noise is white in all channels over frequencies lower than 50 MHz. By increasing N to 40 channels, LF-RIN reaches –128 dB/Hz, as shown in inset (b). Further increase in N induces much enhancement in the LF-RIN level (−92 dB/Hz) as shown in inset (c), which indicates a chaotic-like RIN as manifestation of the completely distorted signal in this case of high load ($N = 80$).

It is interesting to examine the manner in which the laser noise causes a negative impact on CNR of CATV links [2,6,23,33]. Figure 5 compares the relations CNR_{SL} and m/ch for three different number of channels, $N = 25$, 40, and 80. Each value of N is characterised qualitatively by the same character that CNR_{SL} improves equally (on the ground that each channel has the same power) with the increase in m/ch up to a specific maximum value of CNR_{SL} (peak value), and then degrades remarkably. The three peaks of CNR_{SL} (optimum values) shown in the figure correspond to specific values of m/ch. These peak values decrease with

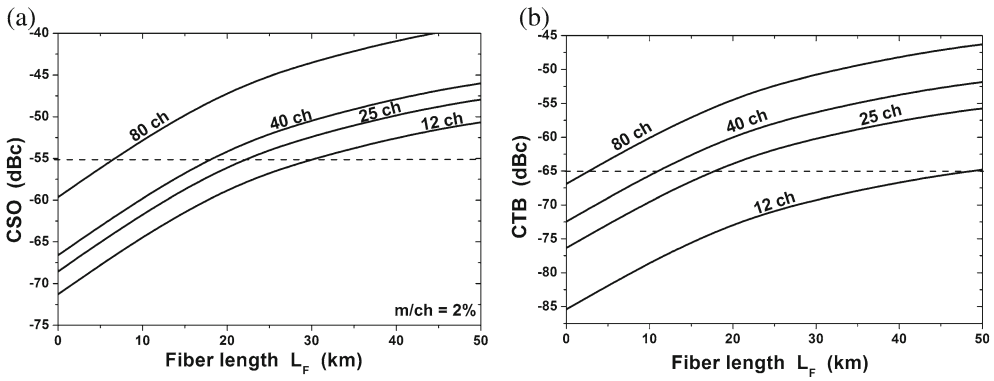

Figure 3. Variation of (**a**) CSO and (**b**) CTB with L_F under 12, 25, 40, and 80 channels when $m/ch = 2\%$ at ch. 12. The dashed lines represent the threshold acceptable levels.

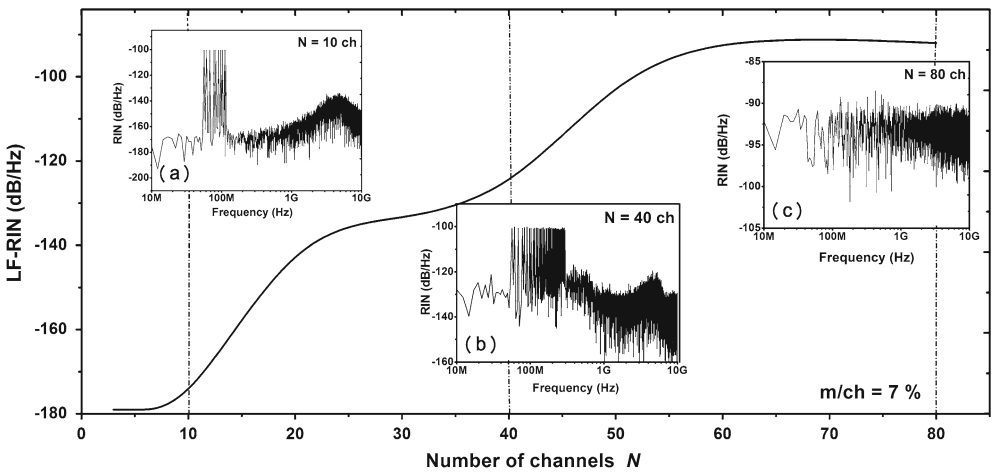

Figure 4. Variation of laser LF-RIN with the number of channels N when $m/ch = 7\%$. The insets are spectra of RIN when $N = 10$, 40, and 80.

the increase in N. The effect of the laser noise appears (CNR_{SL} starts to degrade) at $m/ch > 4\%$ when loading 25 channels, while it appears at $m/ch > 3.5\%$ and $>2\%$ when N increases to 40 and 80, respectively. Beyond the peaks of CNR_{SL}, the higher N have CNR_{SL} values worse than those of lower N. It can be generally summarised that the increase in the number N of loaded channels requires reduction of m/ch in order to ensure acceptable laser noise levels.

The dependencies of the individual noise contributors of the CATV link to the total CNR on m/ch under two different fibre lengths of $L_F = 10$ and 50 km are demonstrated in figure 6. Figures 6a and 6b correspond to loaded channels of number $N = 40$ when $L_F = 10$ and 50 km, respectively. The obtained results reveal that the CNR values coming from the shot noise (CNR_{shot}) and thermal noise ($CNR_{thermal}$) of the receiver improve with the increase in m/ch, which is attributed to an increase in the signal power. Regarding the behaviour of CNR_{SL}, it follows the same behaviours in figure 5. When $L_F = 10$ km, the values of both CNR_{shot} and

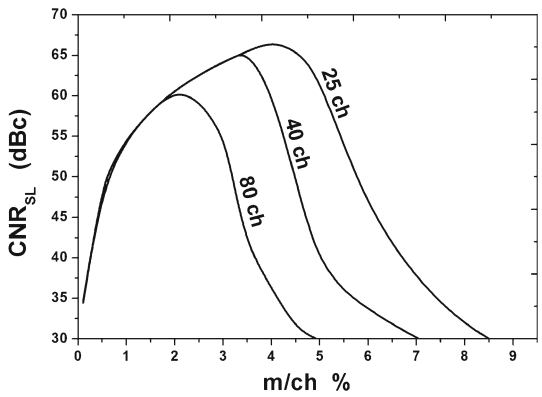

Figure 5. Variation of CNR_{SL} with m/ch under 25, 40, and 80 channels. The three peaks are the optimum values of CNR_{SL}.

$CNR_{thermal}$ are higher than the CNR_{SL} values, as shown in figure 6a, which indicates that the laser noise is the dominant noise source. Increasing L_F up to 50 km makes the thermal noise dominant up to $m/ch \sim 2.5\%$,

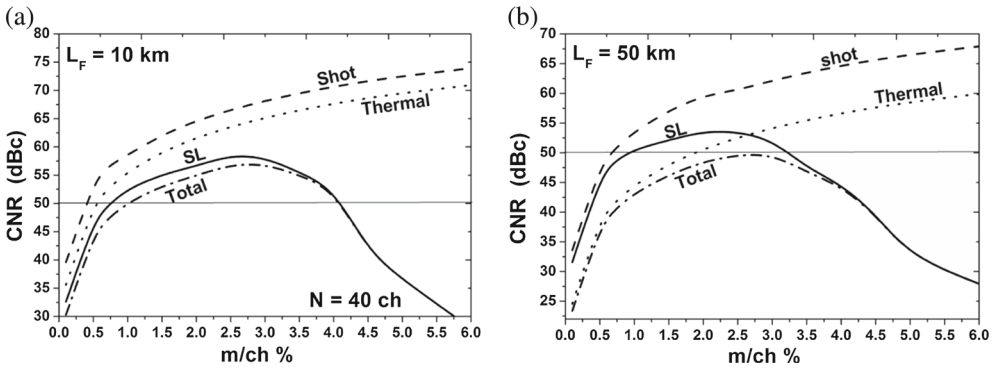

Figure 6. CNR due to laser RIN (solid line), receiver shot noise (dashed line), and thermal noise (dotted line) as well as total link CNR (dash–dotted line) as functions of m/ch when (**a**) L_F = 10 km and (**b**) L_F = 50 km while loading 40 channels. The straight solid line represents the threshold acceptable levels of total link CNR.

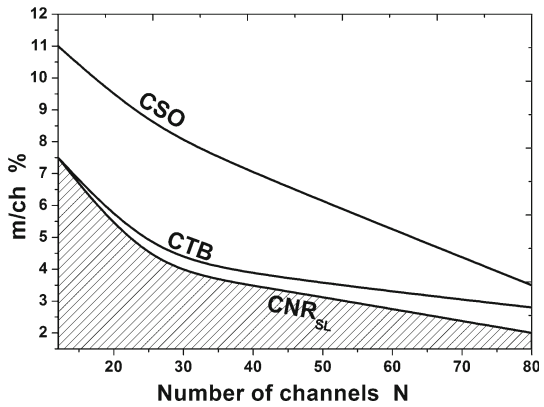

Figure 7. Optimum value of m/ch as a function of the number of channels that correspond to acceptable levels of CSO, CTB, and CNR_{SL} (corresponding to the shadow area).

as shown in figure 6b. Comparing the two figures reveal that the total CNR of the shorter link ($L_F = 10$ km) is higher than that of the longer link ($L_F = 50$ km). Also, based on the threshold acceptable level CNR (>50 dBc) of the total CATV link as reported in [1,6,10] (straight solid line in the two figures), shorter links correspond to wider range of m/ch than longer links.

4.3 *Optimum distortion and noise characteristics*

In order to introduce a more detailed picture on the optimum modulation and design parameters required to achieve best distortion and noise performance of the SL, the predicted optimum ranges of N and m/ch that correspond to acceptable values of CSO, CTB and CNR_{SL} are plotted in figure 7. The figure indicates that the optimum values of m/ch of CNR_{SL} decrease below those of CSO and CTB. This decrease of the maximum m/ch increases with the increase in N. As numeric examples, loading 12 and 80 channels requires values of m/ch = 11% and 3.5% to achieve minimum CSO and of 7.5% and 2.8% to achieve minimum CTB and less than 7.5% and 2% to achieve maximum CNR_{SL}, respectively. As a result, it can be concluded that the optimum values of m/ch vs. the number N of the loaded channels are determined by CNR_{SL}, which corresponds to the shadow area of figure 7.

Figure 8 plots the predicted optimum ranges of N and m/ch that correspond to acceptable values of CSO, CTB, and CNR for the CATV fibre link when (a) $L_F = 10$ km and (b) $L_F = 50$ km. The figure indicates that the optimum ranges of m/ch and

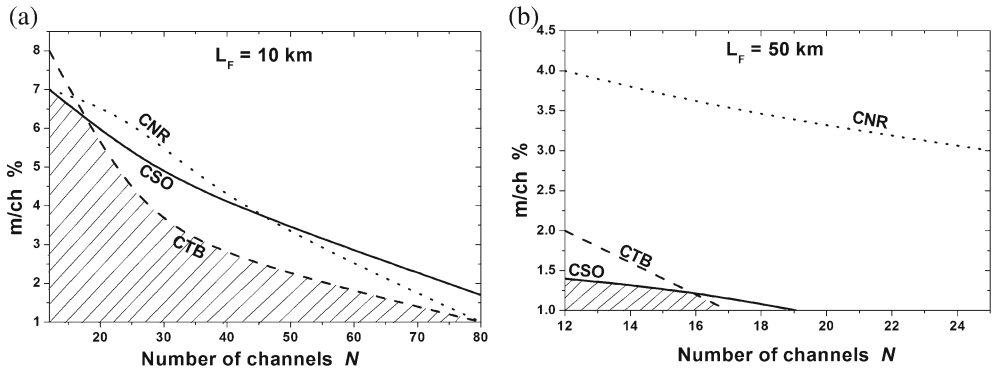

Figure 8. Optimum value of m/ch as a function of N that correspond to acceptable levels of CSO, CTB, and CNR for CATV fibre link when (**a**) $L_F = 10$ km and (**b**) $L_F = 50$ km. The shadow areas correspond to the optimum ranges of m/ch and N.

number of channels N that correspond to best distortion and noise performance for CATV fibre link are determined by the CSO and CTB distortions. When $L_F = 10$ km, the increase in the number of channels from $N = 12$ to 80 corresponds to lowering the optimum value of m/ch, which corresponds to accepted distortion and noise performance from 7 to 1%, which correspond to the shadow area in figure 8a. When $L_F = 50$ km, the optimum value of m/ch is limited between 1.4 and 1%, which corresponds to loading between 12 and 17 channels only as shown in the small shadow area in figure 8b. The present calculations showed that the fibre dispersion did not affect the obtained results up to 50 km fibre length.

5. Conclusions

We introduced numerical modelling and simulation of distortion and noise of SLs and CATV fibre links subject to multichannel modulation. The obtained results showed that both CSO and CTB increase with the increase in m/ch and/or number N of the loaded channels as well as length of the fibre. The maximum value of m/ch required to achieve modulation with maximum values of CNR decreases with the increase of both N and L_F. The laser noise is the dominant noise source in short CATV links (10 km), whereas the thermal noise is the dominant contributor in long links (50 km). Also, shorter links correspond to wider range of m/ch. The ranges of the optimum values of m/ch and N that correspond to accepted values of CSO, CTB, and CNR are narrower in the long CATV fibre link of $L_F = 50$ km than the short link of $L_F = 10$ km.

References

[1] J Lipson, L C Upadhyayula, S Y Huang, C B Roxlo, E J Flynn, P M Nitzsche, C J Mcgrath, G L Fenderson and M S Schaefer, *IEEE Trans. Microw. Theory Technol.* **38**, 483 (1990)

[2] M V Water, *Low-cost CATV transmission in fibre -to-the-home networks,* Master thesis (Eindhoven University of Technology, The Netherlands, 2005)

[3] G P Agrawal, *Fibre-optic communication systems* (John Wiley and Sons Incorporation, New York, 2002) Vol. 222

[4] K Y Lau and A Yariv, *Appl. Phys. Lett.* **45**, 1034 (1984)

[5] H H Lu, Y P Lin and M C Lin, *Opt. Commun.* **22**, 1 (2001)

[6] A Brillant, *Digital and analog fibre optic communications for CATV and FTTx applications* (SPIE Press Monograph, Bellingham, 2008) Vol. PM174

[7] W Ciciora, *An overview: Cable television in the United States* (Cable Television Laboratories, Louisville, 1995)

[8] J Helms, *J. Lightw. Technol.* **10**, 1901 (1992)

[9] T B Warren and J Kouzoujian, *Some notes on composite second and third order intermodulation distortions* (Matrix Test Equipment, 2005) MTN-108

[10] T E Darcie and G E Bodeep, *IEEE Trans. Microw. Theory Technol.* **38**, 524 (1990)

[11] H T Lin and Y H Kao, *IEEE J. Lightwave Technol.* **14**, 2567 (1996)

[12] H B Neo, *Analysis of relative intensity noise and simulation of vertical-cavity surface-emitting lasers*, Ph.D. thesis (University of Queensland, 2001)

[13] W Y Lin, C H Chang, P C Peng, H H Lu and C H Huang, *Opt. Express* **18**, 10301 (2010)

[14] J Chiddix, H Laor, D M Pangrac, L D Williamson and R W Wolfe, *IEEE J. Sel. Areas Commun.* **8**, 1229 (1990)

[15] A Bakry and M Ahmed, *Phys. Wave Phenom.* **24**, 1 (2016)

[16] E E Bergmann, C Y Kuo and S Y Huang, *IEEE Photon. Technol. Lett.* **3**, 59 (1991)

[17] J Koscinski, *Feasibility of multichannel VSB/AM transmission on fibre optic links* (NCTA Technical Papers, 1986)

[18] P J Corvini and T L Koch, *J. Lightwave Technol.* **5**, 1591 (1987)

[19] M Ahmed and A El-Lafi, *Pramana – J. Phys.* **71**, 99 (2009)

[20] Y Y Kia and E Rajaei, *Pramana – J. Phys.* **89**, 37 (2017)

[21] M Ahmed, M Yamada and M Saito, *IEEE J. Quantum Electron.* **37**, 1600 (2001)

[22] K Petermann, *Laser diode modulation and noise* (Springer, The Netherlands, 1988) Vol. 3

[23] *Intermodulation distortion (IMD) measurements using the 37300 series vector network analyzer*, Anritsu, Application Note, 2000

[24] T E Darcie and G E Bodeep, *IEEE Intl. Conf.* **2**, 1004 (1989)

[25] M Ahmed, *Int. J. Num. Model.* **17**, 147 (2004)

[26] C H Cox III, *Analog optical links theory practice* (Cambridge University Press, New York, 2004)

[27] H H Lu, *Fibre broadband network systems* (National Taipei University of Technology, Taiwan, 2010)

[28] C J McGrath, *NCTA Technical Papers* 232 (1989)

[29] D Dobrev and L Jordanova, *Opt. Fibre Technol.* **12**, 196 (2006)

[30] RF and microwave fibre -optic design guide, Agere Systems Inc., Application Note AP01-006OPTO (2011)

[31] R L Burden, J D Faires and A C Reynolds, *Numerical analysis* 2nd edn (Prindle, Weber and Schmidt, Boston, 1981)

[32] J C Cartledge and R C Srinivasan, *J. Lightwave Technol.* **15**, 852 (1997)

[33] H H Lu, C H Chang and P C Peng, *Frontiers in guided wave optics and optoelectronics* (INTECH Open Access Publisher, Taiwan, 2010) Chapter 28